

Possible origin of ferromagnetism in undoped anatase TiO<sub>2</sub>

Haowei Peng, Jingbo Li,\* Shu-Shen Li, and Jian-Bai Xia

State Key Laboratory for Superlattices and Microstructures, Institute of Semiconductors, Chinese Academy of Sciences,  
P.O. Box 912, Beijing 100083, People's Republic of China

(Received 15 December 2008; revised manuscript received 10 February 2009; published 19 March 2009)

Using first-principles electronic structure calculations we find that the titanium vacancy and divacancy may be responsible for the unexpected ferromagnetism in undoped anatase TiO<sub>2</sub>. An isolated titanium vacancy produces a magnetic moment of  $3.5\mu_B$ , and an isolated titanium divacancy produces a magnetic moment of  $2.0\mu_B$ . The origin of the collective magnetic moments is the holes introduced by the titanium vacancy or divacancy in the narrow nonbonding oxygen  $2p_\pi$  band. At the center of the divacancy, an O<sub>2</sub> dimer forms during the relaxation, which lowers the total energy of the system and leads to the decrease in the total magnetic moment due to a hole compensation mechanism. For both the two native defects, the ferromagnetic state is more stable than the antiferromagnetic state.

DOI: 10.1103/PhysRevB.79.092411

PACS number(s): 75.10.-b, 75.50.Pp

Since the discovery of room-temperature ferromagnetism in Co-doped anatase TiO<sub>2</sub>,<sup>1</sup> a lot of attention has been focused on TiO<sub>2</sub> doped with 3d-transition metals.<sup>2</sup> Recently, Venkatesan *et al.*<sup>3</sup> found unexpected magnetism in thin films of HfO<sub>2</sub> without doping. Because neither Hf<sup>4+</sup> nor O<sup>2-</sup> is a magnetic ion and the *d* and *f* shells of the Hf<sup>4+</sup> ion are either empty or full, this phenomenon is termed as “*d*<sup>0</sup> ferromagnetism.”<sup>3</sup> A similar phenomenon exists in another oxide, CaO. According to a density-functional theory (DFT) calculation, Elfimov *et al.*<sup>4</sup> demonstrated that Ca vacancies in CaO can produce local magnetic moments and transform the nonmagnetic CaO into a half-metallic ferromagnet. These discoveries may also introduce a new path to the high-temperature ferromagnetism in TiO<sub>2</sub>. Actually, Hong *et al.*<sup>5</sup> reported that the undoped TiO<sub>2</sub> films deposited on (100) LaAlO<sub>3</sub> substrates are ferromagnetic at room temperature ( $T_C > 400$  K).

There has been a consensus that the ferromagnetism in the oxides mentioned above is induced by native defects. However, debate still exists: cation vacancies and anion vacancies, which of them can produce magnetic moments? On one hand, Coey and co-workers<sup>3,6</sup> suggested that the magnetism in HfO<sub>2</sub> arises from O vacancies: the O vacancies form an impurity band which mixes with the empty Hf 5*d* states, leading to the spin polarization. On the other hand, a first-principles study<sup>7</sup> shows that Hf vacancies can produce magnetic moment whereas O vacancies cannot. For CaO, the ferromagnetism is also attributed to cation vacancies,<sup>4</sup> and the high symmetry is regarded as a key factor for the forming of net magnetic moments. Because of the high symmetry, degenerate molecular orbitals exist, and the two holes related to the Ca vacancy would occupy the molecular orbitals in a triplet state due to the Coulomb repulsion. However, Das Pemmaraju and Sanvito<sup>7</sup> argued that the symmetry driven orbital degeneracy is not a prerequisite for the existence of the high-spin ground state in HfO<sub>2</sub> with Hf vacancies. As regards to TiO<sub>2</sub>, Hong *et al.*<sup>5</sup> stated that the ferromagnetism in the undoped samples originates from O vacancies based on their experiments. They found that the magnetic moments of the film decrease when the annealing time in oxygen atmosphere increases. However, more and more theoretical studies tend to support the cation vacancy inducing the ferromagnetism mechanism.<sup>7-9</sup>

In this Brief Report, we study systematically the electronic structures and magnetic properties of the O vacancy, Ti vacancy, and Ti divacancy in TiO<sub>2</sub>. According to our calculations, the Ti vacancy and divacancy may be the possible origin of the unexpected ferromagnetism in the undoped anatase TiO<sub>2</sub>.

The first-principles calculations are carried out in the local spin-density approximation (LSDA) based on the DFT, as implemented in the Vienna *ab initio* simulation package.<sup>10</sup> The projector augmented wave pseudopotentials<sup>11</sup> are employed to describe the electron-ion interaction. The valence configurations are  $4s^23d^2$  and  $2s^22p^4$  for Ti and O, respectively. A 48-atom  $2 \times 2 \times 2$  supercell in the anatase structure is used. We use a plane-wave basis set with energy cutoff of 400 eV and a  $6 \times 6 \times 6$  Monkhorst-Pack *k* mesh<sup>12</sup> for the Brillouin-zone sampling. The convergence with respect to the energy cutoff and the *k* mesh has been checked. For the structure relaxation, the atomic positions are relaxed until the Hellman-Feynman force is less than 0.01 eV/Å.

In Fig. 1, we plot a conventional unit cell of anatase TiO<sub>2</sub>. For convenience of discussion, we label 5 Ti sites and 12 O sites with letters and numbers. In the rest of this Brief Report, Ti<sup>a</sup> stands for the Ti atom labeled “a” and O<sup>1</sup> stands for the O atom labeled “1” and so on. In the anatase structure, each Ti atom bonds with six O atoms, forming a slightly distorted octahedron, for example, the six O atoms, O<sup>1</sup> to O<sup>6</sup>, surrounding Ti<sup>b</sup> in Fig. 1. Meanwhile, each O atom bonds with two equatorial Ti atoms and one apical Ti atom, which form a planar isosceles trigonal, for example, the three Ti atoms Ti<sup>a</sup>, Ti<sup>b</sup>, and Ti<sup>c</sup> surrounding the O<sup>5</sup> as shown in the figure. Ti-O bonds in the anatase structure can be divided into two kinds: apical bonds with a bond length of 1.972 Å and equatorial bonds with a bond length of 1.924 Å. In Fig. 1, all the bonds parallel with the Ti<sup>b</sup>-O<sup>6</sup> bond are apical, and the rest are equatorial.

First, we calculate three supercells, which contain no vacancy (Ti<sub>16</sub>O<sub>32</sub>), one O vacancy (Ti<sub>16</sub>O<sub>31</sub>), and one Ti vacancy (Ti<sub>15</sub>O<sub>32</sub>). When an O atom is removed, the three nearest Ti atoms move outward by about 0.2 Å with respect to the vacancy site, and the second-nearest O atoms move inward by about 0.1 Å. When a Ti atom is removed, the two apical O atoms move outward by almost 0.6 Å, and the four

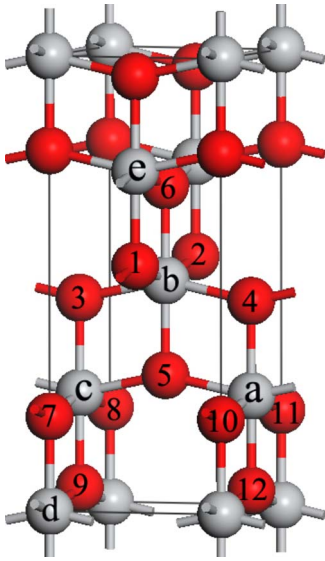


FIG. 1. (Color online) Crystal structure of  $\text{TiO}_2$  in anatase structure. Gray balls represent the Ti atoms and the red (dark) balls represent the O atoms.

equatorial O atoms move outward by only about 0.05 Å. In Fig. 2, we plot the densities of states (DOSs) for  $\text{Ti}_{16}\text{O}_{32}$ ,  $\text{Ti}_{16}\text{O}_{31}$ , and  $\text{Ti}_{15}\text{O}_{32}$ , where the energy scale is aligned according to the atomic core levels. For the perfect anatase  $\text{TiO}_2$  crystal, the DOS is spin unpolarized. The local-density approximation (LDA) band gap is 2.0 eV, which is smaller than the experimental value<sup>13</sup> of 3.2 eV due to the LDA error. For the DOS pattern of the O deficient system, as in a previous study,<sup>14</sup> we find the defect states at the bottom of the conduction band, with a characteristic of Ti 3d orbitals. However, the DOS remains spin unpolarized, and the total magnetic moment of the system is zero. So, according to the LSDA calculation, the O vacancy does not produce a magnetic moment, which disagrees with Hong *et al.*<sup>5</sup> When a Ti vacancy is introduced, the valence band becomes spin polarized as illustrated in Fig. 2(c), and there are hole states above

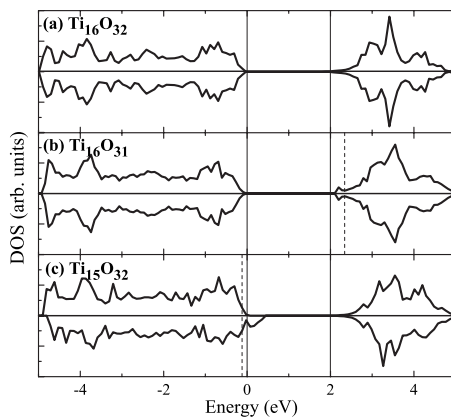


FIG. 2. Spin resolved total DOSs for (a)  $\text{Ti}_{16}\text{O}_{32}$ , (b)  $\text{Ti}_{16}\text{O}_{31}$ , and (c)  $\text{Ti}_{15}\text{O}_{32}$ . Two vertical solid lines indicate the positions of the VBM and conduction-band maximum (CBM) in  $\text{Ti}_{16}\text{O}_{32}$ , and the vertical dotted lines indicate the Fermi energies in corresponding deficient systems.

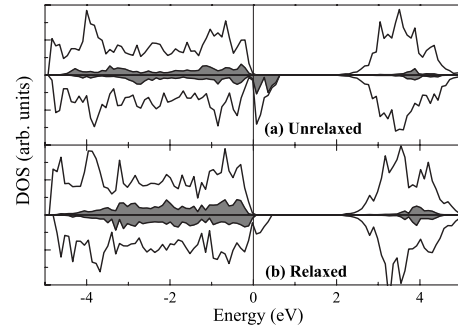


FIG. 3. The spin resolved total DOS (solid lines) and local DOS on the Ti vacancy site (shadow) for Ti deficient supercell  $\text{Ti}_{15}\text{O}_{32}$  (a) before relaxation and (b) after relaxation. The vertical solid line indicates the position of the host VBM.

the host valence-band maximum (VBM). To better understand the nature of the hole states, we perform comparative studies of the relaxed and unrelaxed structures.

For the perfect crystal, the top of the valence band consists mostly of the O  $2p_\pi$  orbitals, which refer to the O  $2p$  orbitals pointing out of the  $\text{Ti}_3\text{O}$  plane.<sup>2,15</sup> When a neutral Ti atom is removed, the Ti vacancy induces four empty states in the narrow O  $2p_\pi$  band because of the 4+ valence state. The magnetic moments per Ti vacancy before and after relaxation are  $4.0\mu_B$  and  $3.5\mu_B$ , respectively. The total DOS and the local DOS at the vacancy site for the unrelaxed and relaxed structures are plotted in Fig. 3. It is shown in the figure that the position of the vacancy-related local DOS shifts to lower energies because of the relaxation. We attribute this shift to the outward relaxation of the neighboring negative charged anions. This transforms the hole states from defect-related ones to host VBM-like ones. To illustrate this change clearly, we plot the wave function squared for the hole states around the vacancy site for the unrelaxed and relaxed Ti deficient supercells. As shown in Fig. 4(a), before relaxation, the holes, and then the magnetic moments, are mostly distributed uniformly over the six O atoms of the  $\text{Ti}^b$ -centered octahedron, i.e.,  $\text{O}^1$  to  $\text{O}^6$ . Whereas after relaxation, the hole states are much more delocalized, which are mainly distributed over the two apical O atoms and their nearest O atoms (such as  $\text{O}^5$  and its nearest O atoms labeled from “3” to “12”), especially the two apical ones, as shown in Fig. 4(b). We can

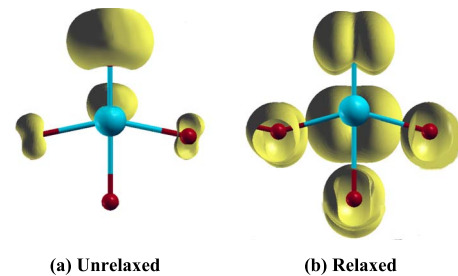


FIG. 4. (Color online) The isosurfaces of charge densities for the minority-spin hole states at  $\Gamma$  point (a) before relaxation and (b) after relaxation in  $\text{Ti}_{15}\text{O}_{32}$ . Let the vacancy takes the site of  $\text{Ti}^b$  in Fig. 1, then the five top layer atoms should be  $\text{O}^3$ ,  $\text{O}^7$ ,  $\text{O}^8$ ,  $\text{O}^9$ , and  $\text{Ti}^c$ , and behind  $\text{Ti}^c$  is  $\text{O}^5$ .

also find that the wave function localized on  $O^3$  and  $O^5$  is distributed symmetrically on the two sides of the  $O^3$ - $Ti^c$ - $O^5$  plane, which is the distinct characteristic of  $O p_\pi$  states.

From the above discussion, we can conclude that the anion vacancies do not change the diamagnetic nature of the anatase  $TiO_2$  crystal. It is the  $Ti$  vacancy that leads to the appearance of a net magnetic moment. In the case of  $CaO^5$ , the high symmetry is considered as a fatal condition for the  $Ca$  vacancy to introduce a  $2.0\mu_B$  magnetic moment. However, from the symmetry consideration, the molecular orbitals are at most threefold degenerate in the crystals. According to the Pauli principle, the possible largest magnetic moment is only  $3\mu_B$ . So the symmetry driven mechanism cannot explain the net magnetization arising from the  $Ti$  vacancy, as in the case of  $HfO_2$ .<sup>7</sup> For  $TiO_2$ , the narrow band comprising nonbonding  $O 2p_\pi$  orbitals at the top of the valence band<sup>2,15</sup> should be responsible for the phenomenon. When a  $Ti$  vacancy is formed, holes are introduced into this narrow band. Basically, spin polarization leads to an exchange splitting of the low energy majority-spin state and high energy minority-spin state. Because there are more electrons in the low energy majority-spin state, this exchange splitting lowers the total energy if holes exist. However, we need narrow bands (or localized states) to avoid the overlaps between the two spin channels, which would reduce or even kill the effect of the exchange splitting. For  $Ti$  deficient  $TiO_2$ , the exchange splitting prevails. Actually, we find that the nonmagnetic state has a higher total energy than the magnetic one by 90.0 meV.

Recently, Ahn *et al.*<sup>16</sup> found that a pair of cation vacancies in rutile  $TiO_2$  and monoclinic  $HfO_2$  is greatly stabilized when the vacancies take the nearest neighboring sites, forming a cation divacancy. In the rutile  $TiO_2$ , an  $O_2$  dimer is formed near the divacancy site. In the anatase  $TiO_2$ , we find a similar phenomenon. As shown in Fig. 1, when the two nearest  $Ti$  atoms  $Ti^a$  and  $Ti^b$  are removed, both  $O^4$  and  $O^5$  bond with only one  $Ti$  atom. After relaxation, the two  $O$  atoms form an  $O_2$  dimer along the  $z$  direction in the center of the divacancy. The  $O^4$ - $O^5$  distance is 1.18 Å, while the bond length in isolated  $O_2$  is 1.22 Å according to the LDA calculation. The stability of the divacancy can be measured by the binding energy which is defined by  $E_b = 2\Delta H(V_{Ti}) - \Delta H(diV_{Ti})$ , where  $\Delta H(V_{Ti})$  and  $\Delta H(diV_{Ti})$  are the formation energies for the single  $Ti$  vacancy and divacancy. The calculated binding energy is as high as 4.875 eV, indicating that the  $Ti$  divacancy is preferred energetically. Meanwhile, the  $Ti$  divacancy has totally different magnetic properties comparing with two isolated single  $Ti$  vacancies. The magnetic moment per divacancy is only  $2.0\mu_B$ . When we put two vacancies at the nearest neighboring sites without structure relaxation, the binding energy and magnetic moment are  $-1.193$  eV and  $7.9\mu_B$ , respectively. So the dramatic drop of the total energy and the total magnetic moment should result from the large structure relaxation and the formation of the  $O_2$  dimer.

It is well known that an isolated  $O_2$  dimer has a ground state with a magnetic moment of  $2\mu_B$ . In Fig. 5, we illustrate schematically the energy levels and their occupation in an  $O_2$  dimer. The magnetic moment arises from the two  $2p$  electrons occupying the double degenerate antibonding  $\pi^*$  orbit-

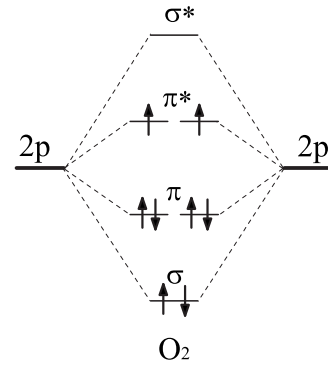


FIG. 5. Schematic diagram for the energy levels of the  $O_2$  dimer and their occupation.  $\sigma$  states are distributed along the  $O_2$  dimer, while the  $\pi$  states are distributed in the plane perpendicular with the dimer.

als. When the dimer is in the  $TiO_2$  matrix, the two  $\pi^*$  electrons will drop to the lower host states, compensating the holes introduced by the  $Ti$  vacancies. Meanwhile, two  $Ti$ - $O$  bonds (as  $Ti^c$ - $O^5$ ) will be broken, resulting in two  $Ti$  dangling bonds.  $Ti$  dangling bonds are essentially the same as  $O$  vacancies, which act as donor defects. These donor defects will further compensate the holes, resulting in a further decreasing of the total magnetic moment. In Fig. 6, we plot the DOS of the supercell containing a  $Ti$  divacancy. In the figure, we also plot the DOS of the antibonding  $\pi^*$  state on the  $O_2$  dimer. It is shown that the  $\pi^*$  state in the spin-up channel is totally unoccupied, so the magnetic moments of the oxygen dimer should be antiparallel with the moments of the surrounding  $O$  atoms. The dotted peak above the Fermi energy in the spin-down channel testifies the charge transfer, i.e., hole compensation. As a result, the local magnetic moments at the  $O_2$  dimer change from  $-2.00\mu_B$  to  $-0.5\mu_B$ , and the total magnetic moments change from  $8.0\mu_B$  to  $2.0\mu_B$ . For the hole distribution on the other  $O$  atoms, it can be derived from the case of single  $Ti$  vacancy doping as shown in Fig. 4(b). However, a correction is needed due to the hole compensation which will decrease the magnetic moments located at the  $O$  atoms near the  $O_2$  dimer and the  $Ti$  dangling bonds.

Now, we have found that the  $Ti$  vacancy and the  $Ti$  divacancy are possibly responsible for the  $d^0$ -ferromagnetism in

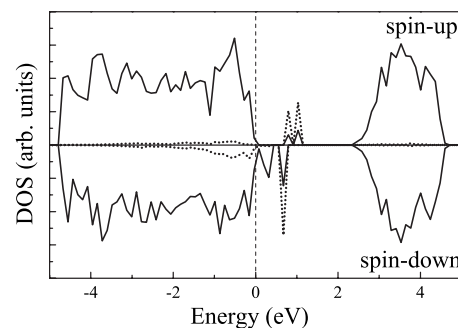


FIG. 6. The spin resolved DOS for the  $Ti_{14}O_{32}$  system, where the two titanium vacancies take the sites of  $Ti^a$  and  $Ti^b$ . The solid line is the total DOS. The dotted line is the DOS of the  $\pi^*$  states localized on the  $O_2$  dimer, as shown in Fig. 5. The Fermi energy is set at zero.

TABLE I. The total-energy difference between the ferromagnetic and antiferromagnetic states,  $\Delta E = E_{\text{FM}} - E_{\text{AFM}}$ . The “sites” are the two sites of the Ti vacancies, as labeled in Fig. 1. The distances between the sites and the total magnetic moments ( $m$ ) for the ferromagnetic states are also tabulated.

Sites	Distance (Å)	$\Delta E$ (meV)	$m$ ( $\mu_B$ )
a, c	3.77	-747	8.0
a, d	4.83	-144	8.0
a, e	5.43	-122	8.0

anatase TiO<sub>2</sub>. In order to investigate the ordering of the magnetic moments around the Ti vacancies, we calculate the total energies of the supercells containing two Ti vacancies, in both the ferromagnetic and antiferromagnetic states. We consider three configurations, where the vacancies take the sites of Ti<sup>a</sup> and Ti<sup>c</sup>, Ti<sup>a</sup> and Ti<sup>d</sup>, and Ti<sup>a</sup> and Ti<sup>e</sup>. Table I summarizes the total-energy differences ( $\Delta E$ ) between the ferromagnetic and antiferromagnetic states and the total magnetic moments of the ferromagnetic state for all the three configurations. The negative  $\Delta E$  suggests that the ferromagnetic ordering is favored energetically. For the divacancies, we calculate the energy difference  $\Delta E$  for a 96 atom supercell containing two divacancies. The ferromagnetic state is also more energetically stable than the antiferromagnetic state by -125 meV. As for the mechanism, it seems similar to the narrow-band ferromagnetism described with a Hubbard model.<sup>17</sup> However, it is still an open problem, and especially, the existence of an O<sub>2</sub> dimer makes it more complicated in the case of divacancy doping.

Because LDA tends to exaggerate delocalization of electron density, we perform LDA+ $U$  calculations as a test with a moderate value of  $U$  (3.6 eV) on the oxygen  $p$  level. We find two changes due to the localization of the hole states: first, the total magnetic moment calculated for the single Ti vacancy increases from  $3.5\mu_B$  to  $4.0\mu_B$ ; second, the ferromagnetic states become more stable. However, the general physical picture is not changed.

In conclusion, the magnetic properties arising from the native defects in anatase TiO<sub>2</sub> have been investigated using the first-principles electronic structure method. O vacancies are not related to the so-called  $d^0$ -ferromagnetism. Ti vacancies produce net magnetic moments, about  $3.5\mu_B$  per vacancy. The origin is the holes introduced by the Ti vacancy in the narrow nonbonding oxygen  $2p_\pi$  band. Ti divacancies also produce net magnetic moments, about  $2.0\mu_B$  per divacancy. When two Ti vacancies take up the nearest sites, an O<sub>2</sub> dimer forms in the center of the divacancy, resulting in the dramatic drop of the total energy and total magnetic moment. For both the magnetic moments arising from the Ti vacancies or divacancies, the ferromagnetic order is preferred energetically.

We thank S.-H. Wei at NREL for helpful discussions. J.L. gratefully acknowledges financial support from “One-hundred Talents Plan” of the Chinese Academy of Sciences. This work was supported by the National Basic Research Program of China (973 Program) under Grant No. G2009CB929300 and the National Natural Science Foundation of China under Grants No. 60821061 and No. 60776061.

\*jbl@semi.ac.cn

<sup>1</sup>Y. Matsumoto, M. Murakami, T. Shono, T. Hasegawa, T. Fukumura, M. Kawasaki, P. Ahmet, T. Chikyow, S. Koshihara, and H. Koinuma, *Science* **291**, 854 (2001).

<sup>2</sup>H. Peng, J. Li, S.-S. Li, and J.-B. Xia, *J. Phys.: Condens. Matter* **20**, 125207 (2008), and references therein.

<sup>3</sup>M. Venkatesan, C. B. Fitzgerald, and J. M. D. Coey, *Nature (London)* **430**, 630 (2004).

<sup>4</sup>I. S. Elfimov, S. Yunoki, and G. A. Sawatzky, *Phys. Rev. Lett.* **89**, 216403 (2002).

<sup>5</sup>N. H. Hong, J. Sakai, N. Poirot, and V. Brizé, *Phys. Rev. B* **73**, 132404 (2006).

<sup>6</sup>J. M. D. Coey, M. Venkatesan, P. Stamenov, C. B. Fitzgerald, and L. S. Dorneles, *Phys. Rev. B* **72**, 024450 (2005).

<sup>7</sup>C. Das Pemmaraju and S. Sanvito, *Phys. Rev. Lett.* **94**, 217205 (2005).

<sup>8</sup>G. Bouzerar and T. Ziman, *Phys. Rev. Lett.* **96**, 207602 (2006).

<sup>9</sup>P. Dev, Y. Xue, and P. Zhang, *Phys. Rev. Lett.* **100**, 117204 (2008).

<sup>10</sup>G. Kresse and D. Joubert, *Comput. Mater. Sci.* **6**, 15 (1996).

<sup>11</sup>G. Kresse and D. Joubert, *Phys. Rev. B* **59**, 1758 (1999).

<sup>12</sup>H. J. Monkhorst and J. D. Pack, *Phys. Rev. B* **13**, 5188 (1976).

<sup>13</sup>S. P. Kowalczyk, F. R. McFreely, L. Ley, V. T. Grstsyna, and D. A. Shirley, *Solid State Commun.* **23**, 161 (1977).

<sup>14</sup>S. Na-Phattalung, M. F. Smith, K. Kim, M.-H. Du, S.-H. Wei, S. B. Zhang, and S. Limpijumnong, *Phys. Rev. B* **73**, 125205 (2006).

<sup>15</sup>R. Asahi, Y. Taga, W. Mannstadt, and A. J. Freeman, *Phys. Rev. B* **61**, 7459 (2000).

<sup>16</sup>H.-S. Ahn, S. Han, and C. S. Hwang, *Appl. Phys. Lett.* **90**, 252908 (2007).

<sup>17</sup>A. Mielke and H. Tasaki, *Commun. Math. Phys.* **158**, 341 (1993).